frontiers in Chemistry

ORIGINAL RESEARCH
published: 17 September 2021
doi: 10.3389/fchem.2021.753617

Theoretical Design of Novel Boron-Based Nanowires *via* Inverse Sandwich Clusters

Cailian Jiang[1], *Zhiwei Lv*[1], *Sudong Lv*[1], *Linwei Sai*[2]*, *Shukai Wang*[1]* and *Fengyu Li*[1]*

[1]School of Physical Science and Technology, Inner Mongolia University, Hohhot, China, [2]College of Science, Hohai University, Changzhou, China

Borophene has important application value, boron nanomaterials doped with transition metal have wondrous structures and chemical bonding. However, little attention was paid to the boron nanowires (NWs). Inspired by the novel metal boron clusters $Ln_2B_n^-$ (Ln = La, Pr, Tb, n = 7–9) adopting inverse sandwich configuration, we examined Sc_2B_8 and Y_2B_8 clusters in such novel structure and found that they are the global minima and show good stability. Thus, based on the novel structural moiety and first-principles calculations, we connected the inverse sandwich clusters into one-dimensional (1D) nanowires by sharing B–B bridges between adjacent clusters, and the 1D-Sc_4B_{24} and 1D-Y_2B_{12} were reached after structural relaxation. The two nanowires were identified to be stable in thermodynamical, dynamical and thermal aspects. Both nanowires are nonmagnetic, the 1D-Sc_4B_{24} NW is a direct-bandgap semiconductor, while the 1D-Y_2B_{12} NW shows metallic feature. Our theoretical results revealed that the inverse sandwich structure is the most energy-favored configuration for transition metal borides Sc_2B_8 and Y_2B_8, and the inverse sandwich motif can be extended to 1D nanowires, providing useful guidance for designing novel boron-based nanowires with diverse electronic properties.

Keywords: first-principles, clusters, inverse sandwich structure, boron-based nanowires, magnetic and electronic properties

OPEN ACCESS

Edited by:
Iwona Anusiewicz,
University of Gdansk, Poland

Reviewed by:
Ke-Qiu Chen,
Hunan University, China
Junjie He,
University of Bremen, Germany
Celina Sikorska,
The University of Auckland, New Zealand

***Correspondence:**
Linwei Sai
sailinwei@hhu.edu.cn
Shukai Wang
wangshukai0323@163.com
Fengyu Li
fengyuli@imu.edu.cn

Specialty section:
This article was submitted to Physical Chemistry and Chemical Physics, a section of the journal Frontiers in Chemistry

Received: *05 August 2021*
Accepted: *30 August 2021*
Published: *17 September 2021*

Citation:
Jiang C, Lv Z, Lv S, Sai L, Wang S and Li F (2021) Theoretical Design of Novel Boron-Based Nanowires via Inverse Sandwich Clusters. Front. Chem. 9:753617. doi: 10.3389/fchem.2021.753617

INTRODUCTION

Boron-based materials were found wide applications in the fileds of emissions, supercapacitors, optical absorptions, photodetectors, *etc.* (Xu et al., 2013; Sussardi et al., 2015; Akopov et al., 2017; Carenco et al., 2013; Tian et al., 2019). Unlike the extensive attention on carbon clusters such as fullerenes and carbon fibers, boron clusters and materials are relatively less studied by scientists. However, there is much space and potential to develop boron-based nanomaterials.

Boron shows a strong tendency to form multi-center-two-electron bonds (mc-2e) in both polyhedral molecules and bulk isotopes (Wang, 2016; Jian et al., 2019; Lipscomb, 1977; Alexandrova et al., 2006) due to its electron deficiency. Therefore, boron clusters have the characteristic of electron delocalization bonding with some delocalized electronic structures and unique aromaticity (Li et al., 2018). In the past two decades, the structure and chemical bonding of bare boron clusters have been studied by combining experimental and theoretical methods (Li et al., 2017; Li et al., 2017; Pan et al., 2019), and planar clusters, nanotube-like cluster structures, graphene-like boron spheres and fullerene-like boron spheres have been found (Kiran et al., 2005; Piazza et al., 2014; Li et al., 2014; Bai et al., 2019; Zhai et al., 2014). Also due to the characteristic of electron deficiency, boron can be doped with metal to form different kinds of metal boride structures. Boron

has formed a large number of important boride materials, ranging from superconducting MgB_2 and superhard transition metal borides to borides with extremely high thermal conductivity (Nagamatsu et al., 2001; Chung et al., 2007).

As the 5th element adjacent to carbon in the periodic table, ring and cage boron clusters have poor stability due to their electron-deficient properties. However, the introduction of transition metals can greatly improve the stability of boron clusters. Transition-metal-doped boron clusters have led to a new direction of boron nanomaterials, such as the metal-centered aromatic borometallic wheels and tubular metal-centered drums (Romanescu et al., 2011; Popov et al., 2015; Jian et al., 2016; Jian et al., 2016; Li et al., 2017). On the other hand, assembling boron clusters by doping them with different types of atoms is a potential way to change properties. For example, CoB_{18}^- and RhB_{18}^- planar clusters have been found, which makes it possible to dope metal with borographene (Li et al., 2016; Jian et al., 2016). Wang and Boldyrev's joint research group have reported a variety of neutral or charged planar wheel clusters centered on supercoordination transition metals M©B_n (M = Fe, Co, Nb, Ru, Rh, Ir, Ta; n = 8–10) (Romanescu et al., 2011).

Recently, Wang's experimental group and Li's theoretical group jointly observed several new metal boron clusters $Ln_2B_n^-$ (Ln = La, Pr, Tb; n = 7–9) with an inverse sandwich structure (Li et al., 2018; Chen et al., 2019). It is found that these clusters have the double aromatic properties of π and σ bonding contributions, showing high stability and symmetry, and the magnetization of B_8^- ring is high. The study provides a novel pattern for the design of new lanthanide borides, and a few inverse sandwich complexes were proposed (Wang et al., 2019; Cui et al., 2020; Shakerzadeh et al., 2020; Xiao et al., 2021). A few questions arise naturally: Would the transition metal borides adopt the inverse sandwich structure in a stable manner? Can the inverse sandwich structure motif be extended to periodic nanomaterials, like designing the super stable 1D-P_{10} nanowire and 2D-P_8N_2 nanosheet based on all pentagon containing P_8 clusters (Wang et al., 2020; Dong et al., 2021)? Thus, in this work, by means of first-principles calculations, we examined the stability of M_2B_8 (M = Sc and Y) clusters with the inverse sandwich structure, and extended the inverse sandwich moiety to design novel boron-based nanowires (NWs). The constructed 1D-Sc_4B_{24} and 1D-Y_2B_{12} NWs show good stability, and the former/later one is a semiconductor/metal. Our theoretical work successfully extended the inverse sandwich moiety to the 1D crystals, which is helpful to design novel boron-based nanowires with diverse electronic properties.

METHODS

The comprehensive genetic algorithm (CGA) (Zhao et al., 2016) combined with the DMol^3 program (Delley, 1990; Delley, 2000) was used to search the global minimum of Sc_2B_8 and Y_2B_8 clusters. The low-energy clusters generated by CGA were further optimized using density functional theory (DFT) implemented in the Vienna *Ab initio* Simulation Package (VASP) code (Kresse and Furthmuller, 1996; Kresse and Hafner, 1993; Kresse and Hafner, 1994). The exchange and correlation functional are defined by the generalized gradient approximation (GGA) with the Perdew–Burke–Ernzerhof (PBE) functional (Perdew et al., 1996). The k points of the geometric optimization and the molecular dynamics simulation were set to $1 \times 7 \times 1$ and $1 \times 3 \times 1$. The phonon spectra were calculated by VASP and Phonopy codes (Togo and Tanaka, 2015). Thermal stability was assessed at 300 and 500 K based on first-principles molecular dynamics [FPMD simulations conducted at the DFT level using a canonical ensemble having a constant number of atoms, volume with the temperature controlled by the Nosé-Hoover thermostat (Martyna et al., 1992; Kresse and Hafner, 1993)], and temperature (NVT) with 1 fs time steps for a total simulated time duration of 5 ps. The band structures of the designed nanowires were calculated by PBE and Heyd-Suseria-Ernzerhof (HSE06) hybrid functional (Heyd et al., 2003). To predict the clusters and nanowires in a more reliable manner, we also considered the PBE + D2 approach (Bučko et al., 2010). Almost no difference was found between the PBE-D2 and PBE structures and cohesive energies.

RESULTS

Structure, Stability and Magnetic Properties of Sc_2B_8 and Y_2B_8 Clusters

Based on the inverse sandwich structure of $La_2B_8^-$, we optimized the neutral transition metal boron clusters of the same configuration—Sc_2B_8 and Y_2B_8 clusters (the two Sc/Y atoms locate symmetrically to the two sides of the B_8 ring). In **Figure 1**, M–B (M = Sc and Y) and B–B bond lengths in two cluster structures are given. For the cluster Sc_2B_8, the bond lengths of Sc–B (d_{Sc-B}) and B–B (d_{B-B}) are 1.68 and 1.62 Å, respectively. For the cluster Y_2B_8, Y–B bond length (d_{Y-B}) is 2.81 Å and the bond length of B–B (d_{B-B}) is 1.62 Å. Both two optimized neutral clusters well preserve the inverse sandwich structure of D_{8h} symmetry.

As shown in **Supplementary Figure S1**, the two vibrational spectra have simple vibration modes due to the high symmetry, and no negative mode was found, indicating the stability of these two clusters. In the Sc_2B_8 cluster, the intensity peaks of 144 and 752 cm^{-1} can be assigned to Sc–B bond and B–B bond vibrations, respectively. The sharp asymmetric oscillations in the Y_2B_8 cluster are at 149 and 721 cm^{-1}, indicating the vibration modes of the Y–B bond and the B–B bond, respectively.

At the same time, a FPMD simulation lasting for 5 ps was performed for both clusters at room temperature (300 K). The annealed structures well remain the original inverse sandwich configuration, as shown in **Supplementary Figure S2**, which also suggests the good stability of the Sc_2B_8 and Y_2B_8 clusters adopting inverse sandwich structure.

Furthermore, CGA was used to generate low-energy isomers of Sc_2B_8 and Y_2B_8 clusters. The four low-lying structures, and an isomer, which can be viewed as the B-centered B_7 ring sandwiched by two Sc/Y atoms, were presented in **Supplementary Figure S3**, and the inverse sandwich configuration for both Sc_2B_8 and Y_2B_8 clusters is the most

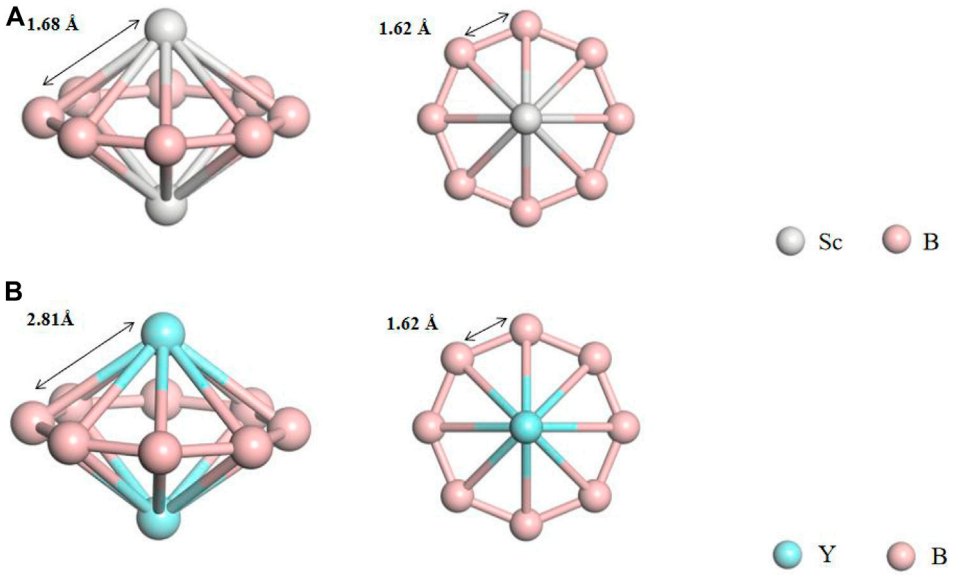

FIGURE 1 | Side and top views of the optimized Sc_2B_8 **(A)** and Y_2B_8 **(B)** clusters.

TABLE 1 | Relative energies of Sc_2B_8 and Y_2B_8 clusters with different magnetic configurations (in eV).

	NM	FM	AFM
Sc_2B_8	0.00	0.00	0.00
Y_2B_8	0.00	0.00	0.00

stable one (0.69–1.34 eV lower than the other four low-energy isomers at PBE-D2 level of theory). In particular, the CCSD(T) test computations also support the PBE-D2 results that the inverse sandwich structures are much lower in energy than other isomers. Thus it is feasible to synthesize the inverse sandwich Sc_2B_8 and Y_2B_8 clusters in experiments.

Additionally, we examined the dissociation of inverse sandwich M_2B_8 (M = Sc, Y) clusters. For the first M dissociation ($M_2B_8 \rightarrow M + MB_8$), the reaction is endothermic by 2.11 and 2.08 eV, respectively for M = Sc and Y; and for removing the second M ($MB_8 \rightarrow M + B_8$), it is also an endothermic reaction with the energy input of 2.37 and 2.17 eV for M = Sc and Y, respectively. The highly endothermic dissociations of M from B_8, indicate reaction barriers are >2 eV. Meanwhile, when the M atoms were put 5 Å from the B_8 center, it will be optimized to the energetically favored inverse sandwich structure. The above results as summarized in **Supplementary Figure S4** again confirmed that the M_2B_8 (M = Sc, Y) clusters with inverse sandwich configuration are highly stable.

Besides, we further explored magnetic properties of the global minimum structures. Three magnetic configurations were compared, namely, antiferromagnetic (AFM), ferromagnetic (FM) and nonmagnetic (NM) states. We set the energy value of NM as 0 eV and all other energy values as their relative differences. Our calculations revealed that both Sc_2B_8 and Y_2B_8 clusters are nonmagnetic (**Table 1**).

Structure and Stability of 1D Nanowires

Considering that the Sc_2B_8 and Y_2B_8 clusters of inverse sandwich configuration are the global minima, the inverse sandwich structural moiety might be extended to a periodic manner. Therefore, we connected the inverse sandwich clusters into 1D nanowires by sharing B–B bridges between adjacent clusters, similar to the observation of inverse triple-decker $La_3B_{14}^-$ (Chen et al., 2019). The 1D-Sc_4B_{24} and 1D-Y_2B_{12} nanowires were obtained after structural relaxation as displayed in **Figure 2**. For the optimized 1D-Sc_4B_{24} (**Figure 2A**), neither the inverse sandwich moiety of Sc_2B_8 nor the sharing B–B bonds was clearly observed, largely due to the formation of B_4 rhombus, which is regarded as a stable unit of boron analogs. The shared B–B (d_{B-B}) key length is ~1.59 Å, and the other B–B (d_{B-B}) lengths are in the range of 1.58–1.62 Å. The Sc–B bond lengths (d_{Sc-B}) are 2.41–2.49 Å. In contrast, for the 1D-Y_2B_{12} NW (**Figure 2B**), the unitcell is formed by two Y_2B_8 clusters of inverse sandwich moiety by sharing a B–B bond. The length of the shared B–B bond ($d_{B\_}B$) is 1.56 Å, the lengths of others B–B bonds are ranged from 1.56 to 1.60 Å. The Y–B bond lengths ($d_{Y\_}B$) are ranged in 2.56–2.72 Å. Compared to the free cluster structures, the $d_{Y\_}B$ were compressed in 1D-Y_2B_{12} nanowire, while the $d_{Sc\_}B$ were significantly stretched in the 1D-Sc_4B_{24}, indicating that although Sc_2B_8 and Y_2B_8 clusters have the same structure, they have different structural characteristics when forming one-dimensional nanowires.

In order to confirm the stability of the two nanowires, we first examined their thermodynamic stability by calculating the cohesive energy (E_{coh}). In our work, the cohesive energy is defined as equation 1, where, E_1/E_2 is the energy of an

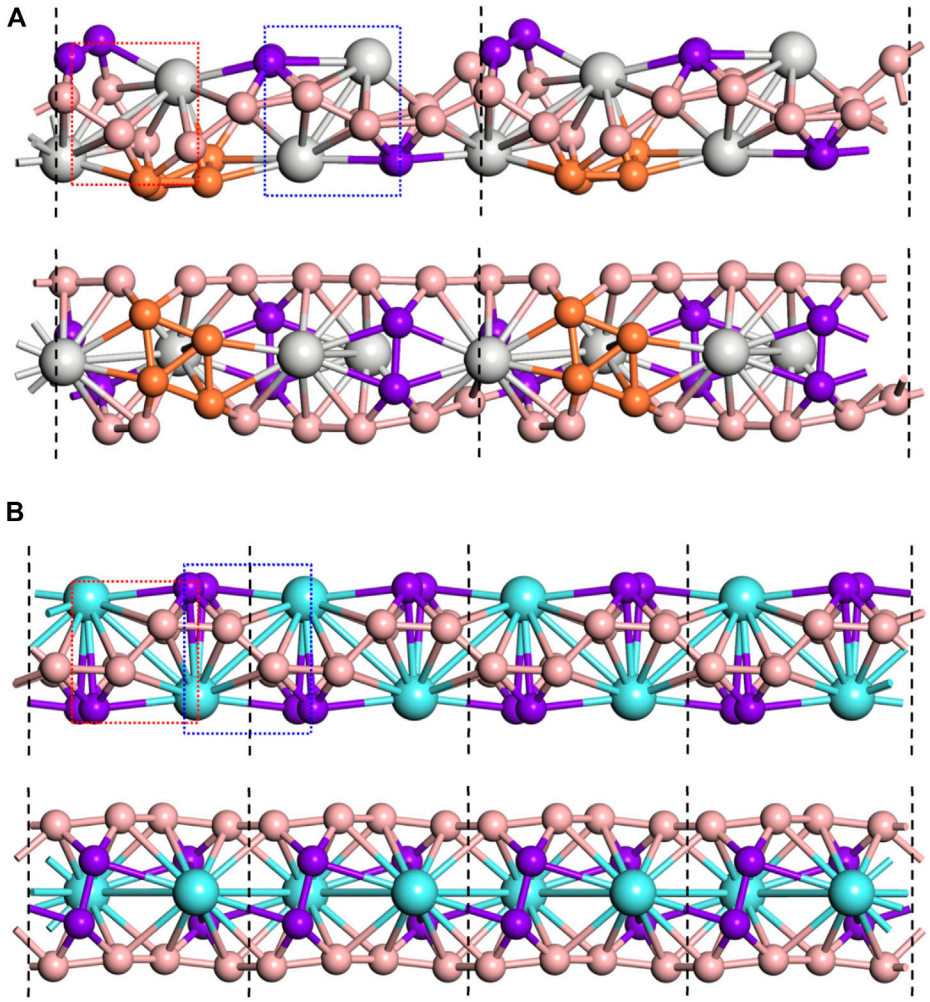

FIGURE 2 | Two views of the 1D-Sc_4B_{24} NW **(A)** and 1D-Y_2B_{12} NW **(B)**. The unitcell was marked by black dashed lines. The inverse sandwich unit M_2B_8 was marked by red and blue dashed rectangle. The sharing B–B bonds and the B rhombus were highlighted in purple and orange, respectively.

isolated transition metal atoms (Sc or Y)/B atom, E_{tot} is the total energy of nanowire, n/m is the number of transition metal/B atoms.

According to the above definition of cohesive energy, the larger the calculated value is, the more stable the structure is. The calculated cohesive energies of 1D-Sc_4B_{24} and 1D-Y_2B_{12} nanowires are 5.92 and 6.00 eV/atom, respectively, much larger than the E_{coh} values of the clusters (5.35 and 5.29 eV/atom, respectively for Sc_2B_8 and Y_2B_8). These high cohesion energies show that two 1D nanowires have good thermodynamic stability.

Then, we calculated the phonon dispersion to investigate their dynamic stability. In these phonon dispersions, no imaginary frequencies were observed (**Figure 3**), indicating that the two designed nanowires based on the inverse sandwich Sc_2B_8 and Y_2B_8 clusters are dynamically stable.

Finally, we performed FPMD simulations in order to access their thermal stability with the supercell of 112 atoms (16 transition metal atoms and 96 B atoms). The 1D-$Sc_{16}B_{96}$ was annealed at 300 K for 5 ps, and the final structure retained the original B_8 rings (**Supplementary Figure S5A**), and the structure obtained remains intact. For the one-dimensional nanowire structure constructed by Y_2B_8, we conducted two 5 ps simulation at room temperature of 300 K (**Supplementary Figure S5B**) and 500 K (**Supplementary Figure S5**), respectively. The 1D-$Y_{16}B_{96}$ structure still showed structural integrity under both simulation conditions. It also preserves structural integrity at 500 K in particular. The results of FPMD simulations confirm that two designed nanowires possess good thermal stability.

Magnetic and Electronic Properties

Through the above analysis of thermodynamic, dynamic and thermal stability, it is found that the two designed nanowires are stable. Therefore, we further explored the magnetic and electronic properties of the two nanowires. For the magnetic

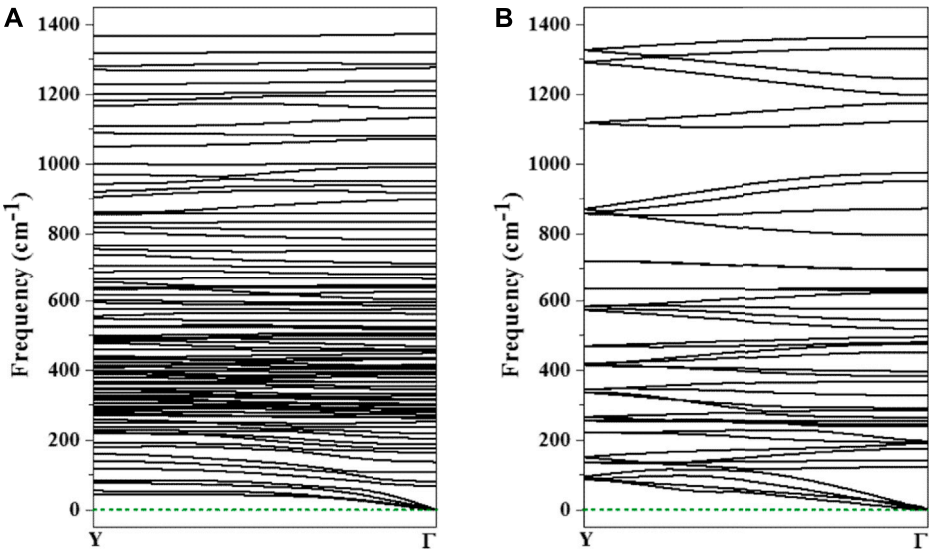

FIGURE 3 | The calculated phonon spectra of the designed 1D-Sc_4B_{24} **(A)** and 1D-Y_2 B_{12} **(B)**.

TABLE 2 | Relative energies of 1D- Sc_4B_{24} and 1D-Y_2B_{12} nanowires with various magnetic configurations (in eV).

	NM	FM	AFM1	AFM2	AFM3
1D-Sc_4B_{24}	0.00	0.00	0.00	0.00	0.00
1D- Y_2B_{12}	0.00	0.00	0.00	0.00	0.00

feature, five magnetic orderings were considered, namely AFM (including AFM1: − + − +, AFM2: + − − +, and AFM3: − − + +, **Supplementary Figure S7**, FM, and NM. Our computations showed that neither 1D-Sc_4B_{24} nor 1D-Y_2B_{12} is magnetic. The relative energies of examined magnetic configurations of the two structures were given in **Table 2**. In addition, through the analysis of charge transfer, we found that each Sc/Y atom transferred ~1.5/2.0 electrons to boron. The differential charge density diagrams of the two 2D nanostructures (**Figure 4**) showed that the electrons have delocalized bonding characteristics.

We used the PBE method to predict the electronic band structures of the two designed nanowires (**Figure 5**). Compared to the metallicity of teetotum cluster Li_2FeB_{14} based nanowire (Shakerzadeh et al., 2020), the 1D-Sc_4B_{24} nanowire is a direct-bandgap semiconductor with the bandgap of 0.51 eV, while the 1D-Y_2B_{12} NW is a metal, and the p orbital of B dominates the state near the Fermi level. The commonly used PBE method usually underestimates the bandgaps. Therefore, we also used HSE06 method to calculate the electronic band structure of 1D-Sc_4B_{24} nanowire, as shown in **Supplementary Figure S8**. The bandgap calculated by the HSE06 method is about 0.85 eV, 0.34 eV larger than the PBE value. The different electronic

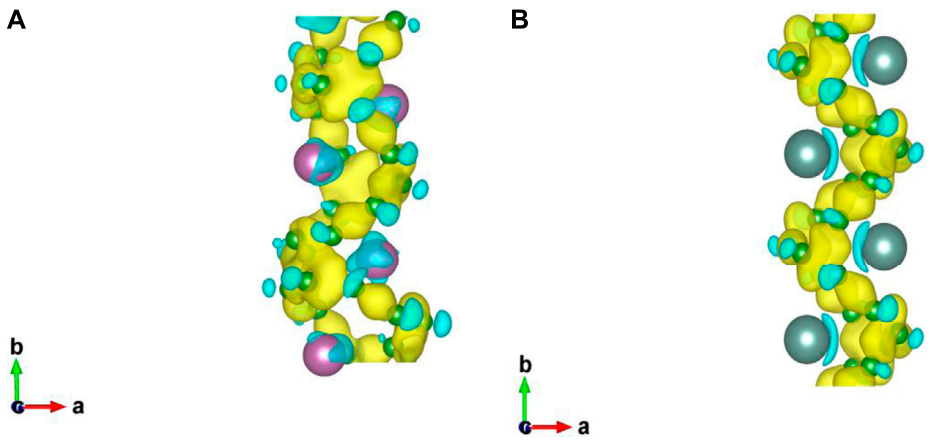

FIGURE 4 | Differential charge density diagrams of designed nanowires 1D-Sc_4B_{24} **(A)** and 1D-Y_2B_{12} **(B)**. The isosurface value was set to be 0.015 e/Bohr^3.

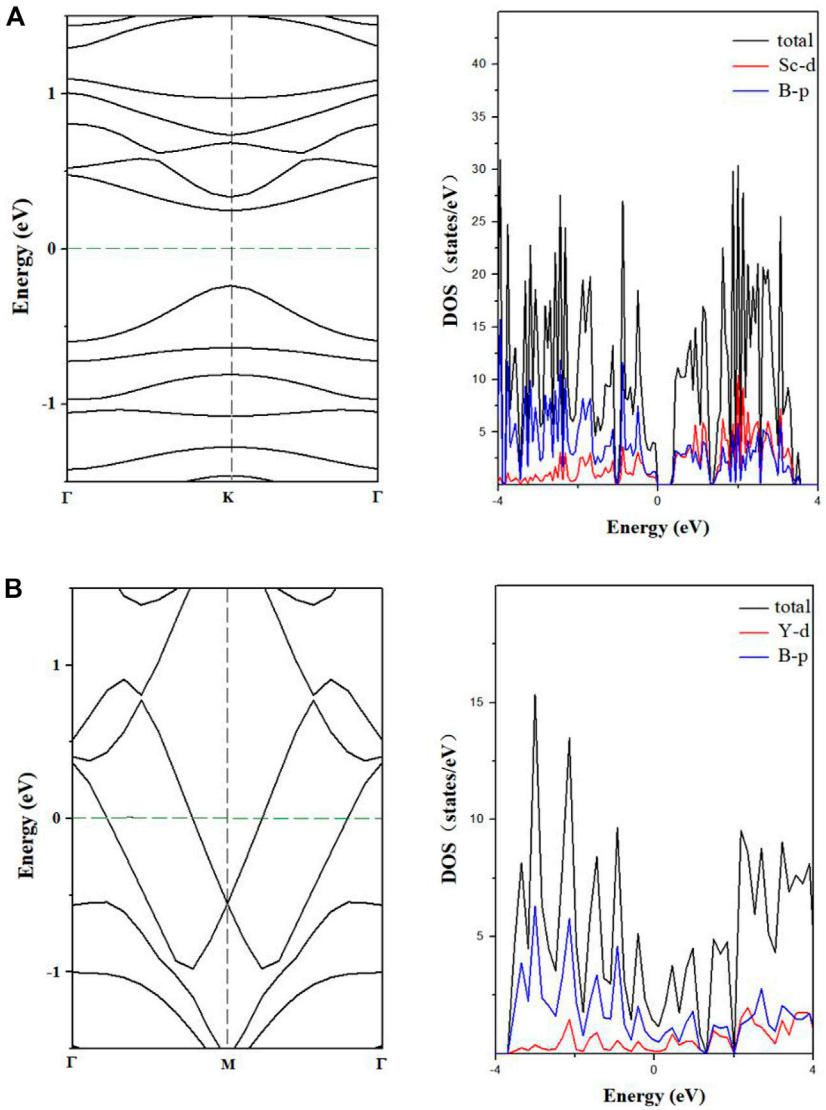

FIGURE 5 | Energy band and density of states of 1D-Sc_4B_{24} **(A)**, 1D-Y_2B_{12} **(B)** nanowires predicted by PBE.

behavior of the two designed nanowires may originate from the different structures (Zeng et al., 2019).

CONCLUSION

In summary, by means of first-principles calculations combined with CGA search, we found that Sc_2B_8 and Y_2B_8 clusters of inverse sandwich structure are the lowest-energy isomers and have good stability, and we constructed one-dimensional nanowires containing the structural moiety of the two clusters. The high stability of 1D-Sc_4B_{24} and 1D-Y_2B_{12} nanowires is confirmed by the investigation of thermodynamical, dynamical and thermal perspectives. Both 1D-Sc_4B_{24} and 1D-Y_2B_{12} nanowires are nonmagnetic; in terms of electronic behavior, the 1D-Sc_4B_{24} is semiconducting with the HSE06 bandgap of 0.85 eV, while the 1D-Y_2B_{12} is metallic. Our theoretical work not only identified the inverse sandwich configuration as the lowest-energy one for transition metal borides Sc_2B_8 and Y_2B_8 clusters, but also successfully extended the inverse sandwich moiety to 1D nanomaterials. Thus, it is helpful to design novel boron-based nanowires for both experimental and theoretical communities.

$$E_{coh} = (nE_1 + mE_2 - E_{tot})/(n+m)$$

Permission to Reuse and Copyright

licenses, to follow any citation instructions requested by third-party rights holders, and cover any supplementary charges.

DATA AVAILABILITY STATEMENT

The original contributions presented in the study are included in the article/**Supplementary Material**, further inquiries can be directed to the corresponding authors.

AUTHOR CONTRIBUTIONS

CJ contributed to calculations, methodology, formal analysis, writing—original draft, and funding acquisition. ZL performed formal analysis and writing—original draft. SL performed data curation and investigation. LS and SW performed methodology, investigation, writing—original draft, and supervision, and funding acquisition. FL contributed to conceptualization, methodology, writing—review and editing, funding acquisition, project administration, and supervision.

FUNDING

This work was supported by the National Natural Science Foundation of China (11964024, 1804076), the "Grassland Talents" project of Inner Mongolia autonomous region (12000-12102613), and the Training Program of Innovation and Entrepreneurship for Undergraduates of Inner Mongolia University (201810126056).

SUPPLEMENTARY MATERIAL

The Supplementary Material for this article can be found online at: https://www.frontiersin.org/articles/10.3389/fchem.2021.753617/full#supplementary-material

REFERENCES

Akopov, G., Yeung, M. T., and Kaner, R. B. (2017). Rediscovering the Crystal Chemistry of Borides. *Adv. Mater.* 29, 1604506. doi:10.1002/adma.201604506

Alexandrova, A. N., Boldyrev, A. I., Zhai, H.-J., and Wang, L.-S. (2006). All-boron Aromatic Clusters as Potential New Inorganic Ligands and Building Blocks in Chemistry. *Coord. Chem. Rev.* 250, 2811–2866. doi:10.1016/j.ccr.2006.03.032

Bai, H., Chen, T.-T., Chen, Q., Zhao, X.-Y., Zhang, Y.-Y., Chen, W.-J., et al. (2019). Planar B41− and B42− Clusters with Double-Hexagonal Vacancies. *Nanoscale* 11, 23286–23295. doi:10.1039/C9NR09522E

Bučko, T., Hafner, J., Lebègue, S., and Ángyán, J. G. (2010). Improved Description of the Structure of Molecular and Layered Crystals: Ab Initio DFT Calculations with van der Waals Corrections. *J. Phys. Chem. A.* 114, 11814–11824. doi:10.1021/jp106469x

Carenco, S., Portehault, D., Boissière, C., Mézailles, N., and Sanchez, C. (2013). Nanoscaled Metal Borides and Phosphides: Recent Developments and Perspectives. *Chem. Rev.* 113, 7981–8065. doi:10.1021/cr400020d

Chen, T.-T., Li, W.-L., Li, J., and Wang, L.-S. (2019). [La(ηx-Bx)La]− (X = 7-9): a New Class of Inverse sandwich Complexes. *Chem. Sci.* 10, 2534–2542. doi:10.1039/C8SC05443F

Chung, H.-Y., Weinberger, M. B., Levine, J. B., Kavner, A., Yang, J.-M., Tolbert, S. H., et al. (2007). Synthesis of Ultra-incompressible Superhard Rhenium Diboride at Ambient Pressure. *Science* 316, 436–439. doi:10.1126/science.1139322

Cui, Z.-H., Chen, C., Wang, Q., Zhao, L., Wang, M.-H., and Ding, Y.-h. (2020). Inverse sandwich Complexes of B7M2−, B8M2, and B9M2+ (M = Zr, Hf): the Nonclassical M-M Bonds Embedded in Monocyclic boron Rings. *New J. Chem.* 44, 17705–17713. doi:10.1039/D0NJ03999C

Delley, B. (1990). An All-electron Numerical Method for Solving the Local Density Functional for Polyatomic Molecules. *J. Chem. Phys.* 92, 508–517. doi:10.1063/1.458452

Delley, B. (2000). From Molecules to Solids with the DMol3 Approach. *J. Chem. Phys.* 113, 7756–7764. doi:10.1063/1.1316015

Dong, Y., Wang, S., Yu, C., Li, F., Gong, J., and Zhao, J. (2021). First-principles Explorations on P8 and N2 Assembled Nanowire and Nanosheet. *Nano Express* 2, 010004. doi:10.1088/2632-959X/abd899

Heyd, J., Scuseria, G. E., and Ernzerhof, M. (2003). Hybrid Functionals Based on a Screened Coulomb Potential. *J. Chem. Phys.* 118, 8207–8215. doi:10.1063/1.1564060

Jian, T., Chen, X., Li, S.-D., Boldyrev, A. I., Li, J., and Wang, L.-S. (2019). Probing the Structures and Bonding of Size-Selected Boron and Doped-boron Clusters. *Chem. Soc. Rev.* 48, 3550–3591. doi:10.1039/C9CS00233B

Jian, T., Li, W.-L., Chen, X., Chen, T.-T., Lopez, G. V., Li, J., et al. (2016). Competition between Drum and Quasi-Planar Structures in RhB18−: Motifs for Metallo-Boronanotubes and Metallo-Borophenes. *Chem. Sci.* 7, 7020–7027. doi:10.1039/C6SC02623K

Jian, T., Li, W.-L., Popov, I. A., Lopez, G. V., Chen, X., Boldyrev, A. I., et al. (2016). Manganese-centered Tubular boron Cluster - MnB16−: A New Class of Transition-Metal Molecules. *J. Chem. Phys.* 144, 154310. doi:10.1063/1.4946796

Kiran, B., Bulusu, S., Zhai, H.-J., Yoo, S., Zeng, X. C., and Wang, L.-S. (2005). Planar-to-tubular Structural Transition in boron Clusters: B20 as the Embryo of Single-Walled boron Nanotubes. *Proc. Natl. Acad. Sci.* 102, 961–964. doi:10.1073/pnas.0408132102

Kresse, G., and Furthmüller, J. (1996). Efficiency of Ab-Initio Total Energy Calculations for Metals and Semiconductors Using a Plane-Wave Basis Set. *Comput. Mater. Sci.* 6, 15–50. doi:10.1016/0927-0256(96)00008-0

Kresse, G., and Hafner, J. (1993). Ab Initiomolecular Dynamics for Liquid Metals. *Phys. Rev. B* 47, 558–561. doi:10.1103/PhysRevB.47.558

Kresse, G., and Hafner, J. (1994). Ab Initiomolecular-Dynamics Simulation of the Liquid-Metal-Amorphous-Semiconductor Transition in Germanium. *Phys. Rev. B.* 49, 14251–14269. doi:10.1103/physrevb.49.14251

Li, W.-L., Chen, Q., Tian, W.-J., Bai, H., Zhao, Y.-F., Hu, H.-S., et al. (2014). The B35 Cluster with a Double-Hexagonal Vacancy: A New and More Flexible Structural Motif for Borophene. *J. Am. Chem. Soc.* 136, 12257–12260. doi:10.1021/ja507235s

Li, W.-L., Chen, T.-T., Xing, D.-H., Chen, X., Li, J., and Wang, L.-S. (2018). Observation of Highly Stable and Symmetric Lanthanide Octa-boron Inverse Sandwich Complexes. *Proc. Natl. Acad. Sci. USA.* 115, E6972–E6977. doi:10.1073/pnas.1806476115

Li, W.-L., Chen, X., Jian, T., Chen, T.-T., Li, J., and Wang, L.-S. (2017). From Planar Boron Clusters to Borophenes and Metalloborophenes. *Nat. Rev. Chem.* 1, 0071. doi:10.1038/s41570-017-0071

Li, W.-L., Hu, H.-S., Zhao, Y.-F., Chen, X., Chen, T.-T., Jian, T., et al. (2018). Recent Progress on the Investigations of boron Clusters and boron-based Materials (I): Borophene. *Sci. Sin.-Chim.* 48, 98–107. doi:10.1360/N032017-00185

Li, W.-L., Jian, T., Chen, X., Li, H.-R., Chen, T.-T., Luo, X.-M., et al. (2017). Observation of a Metal-Centered B2-Ta@B18−tubular Molecular Rotor and a Perfect Ta@B20−boron Drum with the Record Coordination Number of Twenty. *Chem. Commun.* 53, 1587–1590. doi:10.1039/C6CC09570D

Li, W. L., Jian, T., Chen, X., Chen, T. T., Lopez, G. V., Li, J., et al. (2016). The Planar CoB 18 − Cluster as a Motif for Metallo-Borophenes. *Angew. Chem. Int. Ed.* 55, 7358–7363. doi:10.1002/anie.201601548

Lipscomb, W. N. (1977). The Boranes and Their Relatives. *Science* 196, 1047–1055. doi:10.1126/science.196.4294.1047

Martyna, G. J., Klein, M. L., and Tuckerman, M. (1992). Nosé-Hoover Chains: The Canonical Ensemble via Continuous Dynamics. *J. Chem. Phys.* 97, 2635–2643. doi:10.1063/1.463940

Nagamatsu, J., Nakagawa, N., Muranaka, T., Zenitani, Y., and Akimitsu, J. (2001). Superconductivity at 39 K in Magnesium Diboride. *Nature* 410, 63–64. doi:10.1038/35065039

Pan, S., Barroso, J., Jalife, S., Heine, T., Asmis, K. R., and Merino, G. (2019). Fluxional Boron Clusters: From Theory to Reality. *Acc. Chem. Res.* 52, 2732–2744. doi:10.1021/acs.accounts.9b00336

Perdew, J. P., Burke, K., and Ernzerhof, M. (1996). Generalized Gradient Approximation Made Simple. *Phys. Rev. Lett.* 77, 3865–3868. doi:10.1103/PhysRevLett.77.3865

Piazza, Z. A., Hu, H.-S., Li, W.-L., Zhao, Y.-F., Li, J., and Wang, L.-S. (2014). Planar Hexagonal B36 as a Potential Basis for Extended Single-Atom Layer boron Sheets. *Nat. Commun.* 5, 2014. doi:10.1038/ncomms4113

Popov, I. A., Jian, T., Lopez, G. V., Boldyrev, A. I., and Wang, L.-S. (2015). Cobalt-centred boron Molecular Drums with the Highest Coordination Number in the CoB16− Cluster. *Nat. Commun.* 6. doi:10.1038/ncomms9654

Romanescu, C., Galeev, T. R., Li, W.-L., Boldyrev, A. I., and Wang, L.-S. (2011). Aromatic Metal-Centered Monocyclic Boron Rings: CoB8− and RuB9−. *Angew. Chem. Int. Ed.* 50, 9334–9337. doi:10.1002/anie.201104166

Shakerzadeh, E., Duong, L. V., Pham-Ho, M. P., Tahmasebi, E., and Nguyen, M. T. (2020). The Teetotum Cluster Li2FeB14 and its Possible Use for Constructing boron Nanowires. *Phys. Chem. Chem. Phys.* 22, 15013–15021. doi:10.1039/D0CP02046J

Sussardi, A., Tanaka, T., Khan, A. U., Schlapbach, L., and Mori, T. (2015). Enhanced Thermoelectric Properties of Samarium Boride. *J. Materiomics* 1, 196–204. doi:10.1016/j.jmat.2015.07.007

Tian, Y., Guo, Z., Zhang, T., Lin, H., Li, Z., Chen, J., et al. (2019). Inorganic Boron-Based Nanostructures: Synthesis, Optoelectronic Properties, and Prospective Applications. *Nanomaterials* 9, 538. doi:10.3390/nano9040538

Togo, A., and Tanaka, I. (2015). First Principles Phonon Calculations in Materials Science. *Scripta Materialia* 108, 1–5. doi:10.1016/j.scriptamat.2015.07.021

Wang, L.-S. (2016). Photoelectron Spectroscopy of Size-Selected Boron Clusters: From Planar Structures to Borophenes and Borospherenes. *Int. Rev. Phys. Chem.* 35, 69–142. doi:10.1080/0144235X.2016.1147816

Wang, S., Gu, J., Dong, Y., Sai, L., and Li, F. (2020). A Super Stable Assembled P Nanowire with Variant Structural and Magnetic/Electronic Properties via Transition Metal Adsorption. *Nanoscale* 12, 12454–12461. doi:10.1039/D0NR02176H

Wang, Y.-J., Miao, C.-Q., Xie, J.-J., Wei, Y.-R., and Ren, G.-M. (2019). Be2B6 and Be2B7+: Two Double Aromatic Inverse sandwich Complexes with Spin-Triplet Ground State. *New J. Chem.* 43, 15979–15982. doi:10.1039/C9NJ02819F

Xiao, Y., Zhao, X.-K., Wu, T., Miller, J. T., Hu, H.-S., Li, J., et al. (2021). Distinct Electronic Structures and Bonding Interactions in Inverse-Sandwich Samarium and Ytterbium Biphenyl Complexes. *Chem. Sci.* 12, 227–238. doi:10.1039/D0SC03555F

Xu, J., Hou, G., Li, H., Zhai, T., Dong, B., Yan, H., et al. (2013). Fabrication of Vertically Aligned Single-Crystalline Lanthanum Hexaboride Nanowire Arrays and Investigation of Their Field Emission. *NPG Asia Mater.* 5, e53. doi:10.1038/am.2013.25

Zeng, Y. J., Wu, D., Cao, X. H., Zhou, W. X., Tang, L. M., and Chen, K. Q. (2019). Nanoscale Organic Thermoelectric Materials: Measurement, Theoretical Models, and Optimization Strategies. *Adv. Funct. Mater.* 30, 1903873. doi:10.1002/adfm.201903873

Zhai, H.-J., Zhao, Y.-F., Li, W.-L., Chen, Q., Bai, H., Hu, H.-S., et al. (2014). Observation of an All-Boron Fullerene. *Nat. Chem.* 6, 727–731. doi:10.1038/nchem.1999

Zhao, J., Shi, R., Sai, L., Huang, X., and Su, Y. (2016). Comprehensive Genetic Algorithm Forab Initioglobal Optimisation of Clusters. *Mol. Simulation* 42, 809–819. doi:10.1080/08927022.2015.1121386

Conflict of Interest: The authors declare that the research was conducted in the absence of any commercial or financial relationships that could be construed as a potential conflict of interest.

Publisher's Note: All claims expressed in this article are solely those of the authors and do not necessarily represent those of their affiliated organizations, or those of the publisher, the editors and the reviewers. Any product that may be evaluated in this article, or claim that may be made by its manufacturer, is not guaranteed or endorsed by the publisher.